Acta Crystallographica Section B
Structural Science
ISSN 0108-7681

Interplay between dipolar, stacking and hydrogen-bond interactions in the crystal structures of unsymmetrically substituted esters, amides and nitriles of (*R*,*R*)-*O*,*O*′-dibenzoyltartaric acid

Urszula Rychlewska* and Beata Warżajtis

Department of Crystallography, Faculty of Chemistry, Adam Mickiewicz University, Grunwaldzka 6, 60-780 Poznań, Poland

Correspondence e-mail: urszula@krystal.amu.edu.pl

Received 24 January 2001
Accepted 9 March 2001

The compounds analysed are the *O*,*O*′-dibenzoyl derivatives of (*R*,*R*)-tartaric acid, asymmetrically substituted by ester, amide and nitrile groups. Benzoylation does not introduce drastic changes to the molecular conformation. All investigated molecules adopt the planar *T* conformation of the four-carbon chain with noticeably smaller departures from the ideal conformation than observed in the nonbenzoylated analogs. Primary and secondary amides always orient the C═O bond *antiperiplanar* (*a*) with respect to the nearest C*—O bond, while methylester groups adjust their conformation to that adopted by the amide substituent situated at the other end of the molecule. Tertiary amides and carboxyl groups place their carbonyls at the same side as the nearest C*—O bond (the *s* form), but often deviations from coplanarity of the two bonds are significant and higher than those observed in the nonbenzoylated series. The results presented demonstrate the importance of dipole/dipole interactions between CO and βC*H groups in stabilizing the molecular conformation, and between carbonyl groups in stabilizing crystal packing of the molecules that lack classical hydrogen-bond donor groups. An illustration is provided as to how a small change in mutual orientation of molecules arranged in a close-packed fashion causes a change in the character of intermolecular interactions from van der Waals to sandwich stacking between the benzoyloxy phenyls, and to dipolar between the benzoyloxy carbonyls. Hydrogen-bonded molecules tend to orient in a head-to-tail mode; the head-to-head arrangement being limited to cases in which terminal carbonyl groups are situated at one side of the molecule. The orientation of the benzoyloxy substituents with respect to the carbon main chain is such that the (O═)C—O—C—H bond system often deviates significantly from planarity.

1. Introduction

One of the many interesting structural features of (*R*,*R*)-tartaric acid, its esters, amides and salts is the observation that the preference for the planar *T* conformation of the four-atom carbon chain is accompanied by the planarity of α-hydroxycarboxylate or α-hydroxyester or amide moieties as illustrated in Fig. 1 (Gawroński *et al.*, 1997, and references therein). Our previous reports on the subject (Rychlewska *et al.*, 1997; Rychlewska & Warżajtis, 2000*a*) pointed out that stabilization of this conformation might originate from attractive interactions between CO or CN dipoles belonging to the terminal functional groups and C*H dipoles situated at chiral centers at the β position (see Fig. 2*a*). An analogous,

slightly attractive interaction between axial CO and CH bonds has been postulated to exist in inositols (Liang *et al.*, 1994) and in models of C-glycosides (Houk *et al.*, 1993). In small molecules such as propionaldehyde and its homologs, haloalkanes *etc*., the presence of the so-called ^{13}C γ-effect has been explained as resulting from C—H$\cdots n$ interactions between CH groups situated gamma to a heteroatom and a lone pair of electrons at this heteroatom, which lead to the formation of a five-membered chelate ring (Nishio *et al.*, 1998). The system seems analogous to that observed in tartaric acid derivatives, but our model of dipolar interactions rather than C—H$\cdots n$ interactions does not impose geometrical constraints originating from the C—H$\cdots n$ hydrogen-bond formation. In (*R*,*R*)-tartaric acid esters and amides the interacting CO or CN dipoles belong to the terminal carboxyl, ester or amide functions. In *O*,*O*′-dibenzoyl derivatives of (*R*,*R*)-tartaric acid the number of CO dipoles is increased as a result of benzoylation, therefore, it was interesting for us to examine to what extent this will have an effect on the molecular conformation.

O,*O*′-Dibenzoyl and other acyl derivatives of optically active tartaric acid are excellent resolving agents for racemic amines and acid hydrazides, for compounds acting as hydrogen-bond acceptors and for coordination complexes. Therefore, some of the derivatives presented in the paper, for example *O*,*O*′-dibenzoyl-(*R*,*R*)-tartaric acid mono(*N*,*N*-dimethylamide), are used for the resolution of racemic amines (Gawroński & Gawrońska, 1999). From this point of view it was interesting to examine the mode of self-association of these compounds in order to establish the role of particular functional groups in this process, the relationship between conformational and packing preferences and to define the most common packing motifs. Here we report the results of the systematic studies of a series of crystal structures containing asymmetrically substituted *O*,*O*′-dibenzoyl-(*R*,*R*)-tartaric acid derivatives. Here are presented the results of X-ray analysis of eight compounds (see below and Table 1 for the chemical formula of the compounds). The investigated series can be characterized as containing several carbonyl groups in various chemical environments that compete between themselves and with other functional groups in both the intra- and intermolecular interactions.

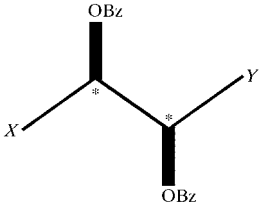

* chiral centres have been marked with asterisks.

(I)

2. Experimental

2.1. Synthesis

The investigated compounds, presented in Table 1, were obtained from the Department of Organic Stereochemistry (formerly the Laboratory of Natural Products), Faculty of Chemistry, Adam Mickiewicz University, Poznań, Poland (Gawroński *et al.*, 1997).

Table 1
The structures discussed.

Abbreviations: numbers 1, 2 and 3 designate primary, secondary and tertiary amide substituents, respectively, while OH, OM, N and C represent hydroxyl, methyl ester, amide and cyano substituents, respectively; B represents benzoylated derivatives.

	X	*Y*	Abbreviation
(*R*,*R*)-(−)-*O*,*O*′-Dibenzoyltartaric acid monoamide	COOH	$CONH_2$	BOH1
(*R*,*R*)-(−)-*O*,*O*′-Dibenzoyltartaric acid mono(*N*-methylamide)	COOH	CONHMe	BOH2
(*R*,*R*)-(−)-*O*,*O*′-Dibenzoyltartaric acid mono(*N*,*N*-dimethylamide)	COOH	$CONMe_2$	BOH3
(*R*,*R*)-(−)-*O*,*O*′-Dibenzoyltartaric acid *N*,*N*-dimethyldiamide	$CONH_2$	$CONMe_2$	BN13
(*R*,*R*)-(−)-*O*,*O*′-Dibenzoyltartaric acid *N*,*N*,*N*′-trimethyldiamide	CONHMe	$CONMe_2$	BN23
(*R*,*R*)-(−)-*O*,*O*′-Dibenzoyltartaric acid monoamide monomethylester	COOMe	$CONH_2$	BOM1
(*R*,*R*)-(−)-*O*,*O*′-Dibenzoyltartaric acid mono(*N*,*N*-dimethylamide) monomethylester	COOMe	$CONMe_2$	BOM3
N,*N*-Dimethyl (2*R*,3*S*)-2,3-dibenzoyloxy-3-cyano-propanamide	CN	$CONMe_2$	BCN3

2.2. X-ray crystallography

Reflection intensities were measured either at room temperature on four-circle Syntex $P2_1$ and KM-4 KUMA Diffraction diffractometers or on a KUMACCD diffractometer at 120 and 150 K. The diffractometers were equipped with graphite monochromators. The background and integrated intensities for reflections measured on a Syntex diffractometer were evaluated from a profile analysis according to Lehmann & Larsen (1974) using the program *PRARA* (Jaskólski, 1982). The intensities were corrected for Lorentz and polarization effects. The structures were solved by direct methods with *SHELXS*86 (Sheldrick, 1990) and refined against F^2 with *SHELXL*97 (Sheldrick, 1997). All non-H atoms were refined anisotropically. The coordinates of the carboxyl and water H atoms, and one of the three H atoms that constitute the *N*-methyl substituent were determined from difference-Fourier maps. The positions of the remaining

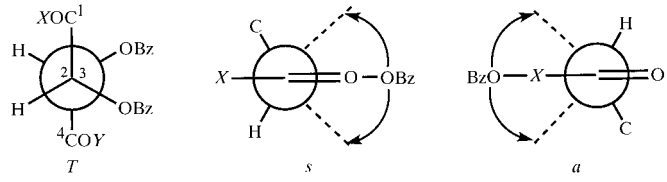

Figure 1
Conformational rotamers characteristic for the presented series of (*R*,*R*)-tartaric acid derivatives. *T* represents the *trans* orientation of the four C atoms that constitute the chain, while *s* and *a* describe the *synplanar* and *antiplanar* orientation of the benzoyloxy oxygen with respect to the nearest carbonyl group.

H atoms were calculated. All H atoms were refined using a riding model and their isotropic displacement parameters were given a value 20% higher than the isotropic equivalent for the atom to which the H atom was bonded, except for the water and carboxyl H atoms in BOH2, as well as the carboxyl hydrogen of the unprimed molecule of BOH1 which were refined isotropically. The carboxyl group of the primed molecule of BOH1 was found to be disordered over two alternative orientations, which could not be fully occupied simultaneously. Thus, the disorder was modeled in the form of a major (primed) and minor (atoms labeled with the letter *a*) component, the occupancy factor refining to 0.70 for the major component. The model for the minor component contained the solvent water molecule. Anisotropic displacement parameters were applied only for atoms of the major occupancy. The absolute structure of the crystals was assumed from the known absolute configuration of (*R*,*R*)-tartaric acid. A Siemens (1989) Stereochemical Workstation was used to prepare the drawings. Crystal data and details of data collection and structure refinement are summarized in Table 2.[1]

3. Results and discussion

*ORTEP*II (Johnson, 1976) drawings of the asymmetric units with numbering schemes are given in Fig. 3. Selected torsion angles are listed in Table 3 and pseudo-torsion angles describing a relative orientation of local dipoles are given in Table 4. The χ_N, χ_C and τ parameters describing the planarity of the *N*,*N*′-dimethylamide group are listed in Table 5. Hydrogen-bond parameters are summarized in Table 6. Parameters describing the geometry of carbonyl dipole/dipole interactions are given in Table 7.

3.1. Structural characteristics of unsymmetrically substituted *O*,*O*′-dibenzoyl-(*R*,*R*)-tartaric acid esters, nitriles and amides

3.1.1. Conformation around the C*—C* bond. For all compounds reported in this paper, as for the optically active tartaric acid, the conformation found in the solid state by X-ray diffraction techniques is staggered, with a planar carbon chain and with the carboxyl or ester or nitrile groups in *trans* (*T*) orientation with respect to the amide group (Fig. 1, Table 3). Among the dibenzoyl derivatives studied so far by X-ray techniques, we have found only two exceptions to this conformation, namely the *O*,*O*′-dibenzoyl-(*R*,*R*)-hydrogen tartrate anion (Hommeltoft *et al.*, 1986) and *O*,*O*′-dibenzoyl-(*R*,*R*)-*N*,*N*′-tetramethyl tartramide (Rychlewska, 1992), both of which adopt in the solid state the *minus gauche* (G^-) conformation. While in the *O*,*O*′-(*R*,*R*)-dibenzoyl-hydrogen tartrate anion the conformation is stabilized by an intramolecular hydrogen bond between the carboxyl and carboxylate groups in the mutual *gauche* orientation, its presence in the structures of *N*,*N*′-tetraalkyltartramides (Gawroński *et al.*, 1989) is probably caused by steric factors. Namely, the presence of the *N*,*N*-dimethylamide group in the molecule with a *T* conformation is a source of steric repulsion between the H atom attached to the chiral center and the methyl H atoms belonging to the dimethylamide group. The presence of two *N*,*N*-dimethylamide groups at both ends of the molecule causes a change in conformation of the main chain from *T* to G^-. The *plus gauche* (G^+), *i.e.* where two OBz substituents are *trans*, is as yet unreported in the crystalline state.

3.1.2. Conformation around the C—C* bond. Tartaric acids and tartrate ions have long been viewed as consisting of two planar halves containing hydroxyacetic acid groups. The planarity of these groups has been discussed in the literature (Kroon, 1982) with the conclusion that the presence of the intramolecular hydrogen bond which stabilizes this conformation is not a necessary condition for it to occur. As follows from our investigations, this generalization can be extended to esters and primary or secondary amides of (*R*,*R*)-tartaric acid (Rychlewska & Warżajtis, 2000*a*) and to the dibenzoylated derivatives thereof. In the reported series, the *T* conformer has the C*—O bond situated in-plane or virtually in-plane of the proximal carboxyl, amide or ester group, in spite of the absence of an intramolecular hydrogen bond in the latter group. In the α-benzoyloxymethylester residue there is no clear tendency for one of the two carbon–oxygen bonds that constitute the methyl ester group to eclipse the nearest C*—O bond [compare the values of the O=C—C*—O torsion angles −158.0 (2) and 15.8 (3)° for BOM1 and BOM3, respectively]. On the other hand, in the α-benzoyloxy amide or methylamide moiety it is always the N—H bond that eclipses the nearest C*—O bond, as indicated by the values of the O=C—C*—O torsion angles that approximate 180° (Table 3). This is contrasted with the α-benzoyloxy carboxyl or *N*,*N*-dimethylamide residues where either the carbonyl bond eclipses the proximal C*—O bond or (more often) the fragment becomes significantly nonplanar, the O=C—C*—O torsion angle approaching the value of 30° (Table 3). The conformation, in which the carbonyl group eclipses the nearest C*—O bond, is described as *synplanar* (*s*), and that in which the carbonyl group is on the opposite side of the proximal C*—O bond is called *antiplanar* (*a*) (Fig. 1). Inspection of the C—C*—C*—C

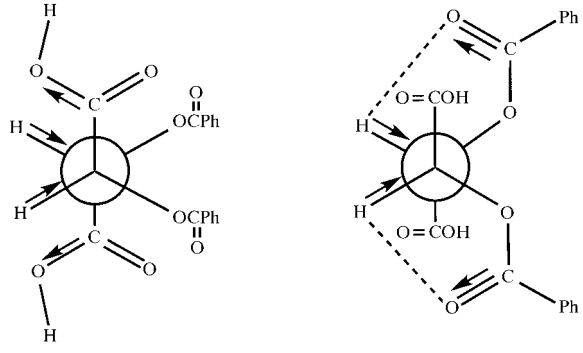

Figure 2
Possible local dipole/dipole interactions (dipoles marked with arrows) and C—H···O intramolecular hydrogen bonds (dashed lines) in *O*,*O*′-dibenzoyl-(*R*,*R*)-tartaric acid and its derivatives possessing the *T* conformation.

[1] Supplementary data for this paper are available from the IUCr electronic archives (Reference: NA0118). Services for accessing these data are described at the back of the journal.

Table 2
Experimental details.

	BOH1	BOH2	BOH3	BN13
Crystal data				
Chemical formula	$C_{18}H_{15}NO_7 \cdot 0.15H_2O$	$C_{19}H_{17}NO_7 \cdot H_2O$	$C_{20}H_{19}NO_7$	$C_{20}H_{20}N_2O_6$
Chemical formula weight	360.01	389.35	385.36	384.38
Cell setting, space group	Monoclinic, $P2_1$	Orthorhombic, $P2_12_12_1$	Orthorhombic, $P2_12_12_1$	Orthorhombic, $P2_12_12_1$
a, b, c (Å)	7.3930 (4), 19.950 (1), 12.1630 (6)	8.7977 (8), 10.752 (1), 20.177 (2)	8.6699 (6), 12.0105 (7), 18.657 (1)	8.9153 (6), 11.758 (1), 17.976 (1)
β (°)	97.770 (4)	90	90	90
V (Å^3)	1777.45 (16)	1908.6 (3)	1942.8 (2)	1884.4 (2)
Z	4	4	4	4
D_x (Mg m^{-3})	1.345	1.355	1.318	1.355
Radiation type	Mo $K\alpha$	Cu $K\alpha$	Mo $K\alpha$	Mo $K\alpha$
No. of reflections for cell parameters	4754	40	8260	3684
θ range (°)	–	12.8–23.9	–	–
μ (mm^{-1})	0.105	0.907	0.101	0.101
Temperature (K)	120 (2)	293 (2)	120 (2)	150 (2)
Crystal form, color	Prism, colorless	Prism, colorless	Prism, colorless	Plate, colorless
Crystal size (mm)	0.25 × 0.20 × 0.20	0.3 × 0.2 × 0.1	0.5 × 0.2 × 0.1	0.40 × 0.20 × 0.05
Data collection				
Diffractometer	Kuma KM4CCD κ-geometry	KM-4 four circle	Kuma KM4CCD κ-geometry	Kuma KM4CCD κ-geometry
Monochromator	Graphite	Graphite	Graphite	Graphite
Data collection method	ω scans	θ–2θ scans	ω scans	ω scans
No. of measured, independent and observed parameters	11 340, 4144, 2463	3086, 2841, 2522	19 283, 2726, 2444	12 108, 2545, 1697
Criterion for observed reflections	$I > 2\sigma(I)$	$I > 2\sigma(I)$	$I > 2\sigma(I)$	$I > 2\sigma(I)$
R_{int}	0.0472	0.0125	0.0726	0.0691
θ_{max} (°)	27.48	67.85	28.28	28.28
Range of h, k, l	$-9 \rightarrow h \rightarrow 6$ $-22 \rightarrow k \rightarrow 25$ $-14 \rightarrow l \rightarrow 15$	$-9 \rightarrow h \rightarrow 9$ $0 \rightarrow k \rightarrow 12$ $0 \rightarrow l \rightarrow 24$	$-11 \rightarrow h \rightarrow 11$ $-8 \rightarrow k \rightarrow 16$ $-24 \rightarrow l \rightarrow 24$	$-8 \rightarrow h \rightarrow 11$ $-15 \rightarrow k \rightarrow 15$ $-22 \rightarrow l \rightarrow 23$
No. and frequency of standard reflections	–	2 every 100 reflections	–	–
Intensity decay (%)	0	2.8	0	0
Refinement				
Refinement on	F^2	F^2	F^2	F^2
$R[F^2 > 2\sigma(F^2)]$, $wR(F^2)$, S	0.0381, 0.072, 0.842	0.0275, 0.0755, 1.079	0.0509, 0.1173, 1.129	0.049, 0.0992, 0.977
No. of reflections and parameters used in refinement	4144, 489	2841, 266	2726, 257	2545, 253
H-atom treatment	Mixed	Mixed	Mixed	Mixed
Weighting scheme	$w = 1/[\sigma^2(F_o^2) + (0.0337P)^2]$, where $P = (F_o^2 + 2F_c^2)/3$	$w = 1/[\sigma^2(F_o^2) + (0.0425P)^2 + 0.1715P]$, where $P = (F_o^2 + 2F_c^2)/3$	$w = 1/[\sigma^2(F_o^2) + (0.0639P)^2 + 0.0000P]$, where $P = (F_o^2 + 2F_c^2)/3$	$w = 1/[\sigma^2(F_o^2) + (0.0471P)^2 + 0.0000P]$, where $P = (F_o^2 + 2F_c^2)/3$
$(\Delta/\sigma)_{max}$	0.000	0.000	0.000	0.000
$\Delta\rho_{max}$, $\Delta\rho_{min}$ (e Å^{-3})	0.151, −0.158	0.116, −0.127	0.223, −0.198	0.169, −0.226
Extinction method	None	*SHELXL*93 (Sheldrick, 1993)	None	None
Extinction coefficient	–	0.0052 (3)	–	–

	BN23	BOM1	BOM3	BCN3
Crystal data				
Chemical formula	$C_{21}H_{22}N_2O_6$	$C_{19}H_{17}NO_7$	$C_{21}H_{21}NO_7$	$C_{20}H_{18}N_2O_5$
Chemical formula weight	398.41	371.34	399.39	366.36
Cell setting, space group	Monoclinic, $P2_1$	Orthorhombic, $P2_12_12_1$	Monoclinic, $P2_1$	Monoclinic, $P2_1$
a, b, c (Å)	8.901 (1), 11.272 (1), 10.414 (1)	7.193 (1), 14.515 (2), 18.083 (2)	8.127 (1), 14.109 (2), 8.733 (1)	7.749 (2), 14.144 (4), 9.063 (2)
β (°)	99.47 (1)	90	97.97 (1)	110.34 (2)
V (Å^3)	1030.62 (18)	1888.0 (4)	991.7 (2)	931.4 (4)
Z	2	4	2	2
D_x (Mg m^{-3})	1.284	1.306	1.338	1.306
Radiation type	Mo $K\alpha$	Mo $K\alpha$	Cu $K\alpha$	Mo $K\alpha$
No. of reflections for cell parameters	30	38	25	15
θ range (°)	8.36–11.25	11.45–13.94	11.98–19.85	5.95–17.34
μ (mm^{-1})	0.095	0.101	0.848	0.095

Table 2 (continued)

	BN23	BOM1	BOM3	BCN3
Temperature (K)	293 (2)	293 (2)	293 (2)	293 (2)
Crystal form, color	Prism, colorless	Prism, colorless	Plate, colorless	Plate, colorless
Crystal size (mm)	0.6 × 0.3 × 0.3	0.7 × 0.6 × 0.6	0.8 × 0.4 × 0.3	0.5 × 0.4 × 0.4
Data collection				
Diffractometer	KM-4 four circle	KM-4 four circle	KM-4 four circle	Syntex $P2_1$
Monochromator	Graphite	Graphite	Graphite	Graphite
Data collection method	θ–2θ scans	θ–2θ scans	θ–2θ scans	θ–2θ scans
No. of measured, independent and observed parameters	4029, 2127, 1752	3976, 2145, 1709	3222, 3110, 3016	3921, 2129, 1423
Criterion for observed reflections	$I > 2\sigma(I)$	$I > 2\sigma(I)$	$I > 2\sigma(I)$	$I > 2\sigma(I)$
R_{int}	0.0158	0.0145	0.0298	0.0331
θ_{max} (°)	26.05	26.06	64.93	27.57
Range of h, k, l	$-11 \rightarrow h \rightarrow 10$ $-13 \rightarrow k \rightarrow 13$ $0 \rightarrow l \rightarrow 12$	$-8 \rightarrow h \rightarrow 8$ $0 \rightarrow k \rightarrow 17$ $0 \rightarrow l \rightarrow 22$	$-9 \rightarrow h \rightarrow 9$ $-16 \rightarrow k \rightarrow 16$ $-10 \rightarrow l \rightarrow 0$	$0 \rightarrow h \rightarrow 9$ $-17 \rightarrow k \rightarrow 17$ $-11 \rightarrow l \rightarrow 11$
No. and frequency of standard reflections	2 every 100 reflections	3 every 100 reflections	2 every 100 reflections	2 every 100 reflections
Intensity decay (%)	1.9	2.1	0.8	4.4
Refinement				
Refinement on	F^2	F^2	F^2	F^2
$R[F^2 > 2\sigma(F^2)]$, $wR(F^2)$, S	0.0305, 0.0837, 1.039	0.0315, 0.0897, 1.045	0.0326, 0.0893, 1.062	0.0435, 0.1065, 1.005
No. of reflections and parameters used in refinement	2127, 262	2145, 244	3110, 263	2129, 245
H-atom treatment	Mixed	Mixed	Mixed	Mixed
Weighting scheme	$w = 1/[\sigma^2(F_o^2) + (0.0444P)^2 + 0.1280P]$, where $P = (F_o^2 + 2F_c^2)/3$	$w = 1/[\sigma^2(F_o^2) + (0.0534P)^2 + 0.1331P]$, where $P = (F_o^2 + 2F_c^2)/3$	$w = 1/[\sigma^2(F_o^2) + (0.0624P)^2 + 0.0749P]$, where $P = (F_o^2 + 2F_c^2)/3$	$w = 1/[\sigma^2(F_o^2) + (0.0503P)^2 + 0.0920P]$, where $P = (F_o^2 + 2F_c^2)/3$
$(\Delta/\sigma)_{max}$	0.000	0.000	0.000	0.000
$\Delta\rho_{max}$, $\Delta\rho_{min}$ (e Å^{-3})	0.142, −0.132	0.127, −0.119	0.166, −0.169	0.123, −0.121
Extinction method	None	None	*SHELXL*93 (Sheldrcik, 1993	*SHELXL*93 (Sheldrcik, 1993
Extinction coefficient	–	–	0.0221 (12)	0.036 (5)

Computer programs used: *Kuma KM4CCD software* (Kuma Diffraction, 1999*a*), *SHELXS*86 (Sheldrick, 1990), *SHELXL*97 (Sheldrick, 1997), *Kuma KM-4 software* (Kuma Diffraction, 1991), SYNTEX Operation Manual, SYNTEX *XTL* Operation Manual, *PRARA* (Syntex, 1973), *KM4RED* (Kuma Diffraction, 1999*b*), *DATAPROC* (Gałdecki *et al.*, 1995), *PRARA* (Jaskólski, 1982).

and O═C—C*—O torsion angles, listed in Table 3, shows that the overall conformation of the investigated molecules can be described as BOH1: *Ts*,*a* (two independent molecules); BOH2: *Ts*,*a*; BOH3: *Ts*,*s*; BN13: *Ta*,*s*; BN23: *Ta*,*s*; BOM1: *Ta*,*a*; BOM3: *Ts*,*s*; BCN3: *Ts*. The molecular conformations are illustrated in Fig. 3. It is interesting to note a change in conformation around the Csp^3—Csp^2 bond within the α-benzoyloxymethylester residue that follows a change in conformation of the α-benzoyloxyamide moiety situated at the other end of the molecule (compare BOM1 and BOM3 molecular conformations, illustrated in Fig. 3, and the corresponding torsion angle values listed in Table 3). Nonplanarity of the O═C—C*—O fragments seem to originate from intermolecular hydrogen-bond interactions (*see below*, Table 6), *i.e.* the carboxyl groups are no longer coplanar with the proximal C*—O bond if they are involved in intermolecular hydrogen bonds as both donors and acceptors. Similarly, dimethylamide substituents significantly increase their inherent tendency for nonplanarity of the O—C*—C(O)NMe_2 fragment (*see above*) if they act as acceptors of intermolecular hydrogen bonds.

3.1.3. Factors stabilizing the molecular conformation. As mentioned in the *Introduction*, the conformation in which a molecule of (*R*,*R*)-tartaric acid or its derivative consists of two planar O—C—C*—O or N—C—C*—O moieties is stabilized by local CO/βC*H (or CN/βC*H) dipolar interactions (see Fig. 2*a*). Consequently, significant nonplanarity of these fragments indicates that dipolar interactions which involve terminal groups no longer operate. However, as these interactions become geometrically less favorable, the C*—H dipoles situated at chiral centers tend to orient nearly parallel to the carbonyl groups belonging to benzoyloxy substituents (Table 4). This creates geometrical conditions favoring dipolar interactions between C*—H dipoles located at chiral centers and benzoyloxy carbonyls attached to the same chiral atom (see Fig. 2*b*). Contrary to the dipolar interactions involving terminal functional groups, the dipolar interactions with the benzoyloxy carbonyl as one of the constituents can, on geometrical grounds, always be classified as the intramolecular C*—H···O hydrogen bonds (compare Tables 4 and 6). This is understandable in view of the fact that in the former bond system the atom that bridges the pair of interacting dipoles is the sp^3 hybridized carbon, while in the latter bond system it is the ether oxygen. From our observations it follows that simultaneous realisation, by the same C*—H bond, of both types of dipolar interactions (as observed for example in

BN23, Table 4) is rarely achieved and dipolar interactions with terminal CO groups are favored over the analogous interactions with the benzoyloxy carbonyls. However, as the former type of dipolar interaction becomes difficult to achieve due to the presence of methyl substituents, the second type of dipolar interactions begins to operate. As can be seen from Table 4, in BN13 and BOM1 the CO components of the interacting CO/βC*—H dipoles belong to the primary amide groups, in BOH1, BOH2 and BN23 they constitute part of both the amide and the benzoyloxy substituents, and in BOH3 belong to both the carboxyl and the benzoyloxy fragments. Considering assumptions usually made when interpreting circular dichroism results (Gawroński *et al.*, 1997), an eclipsed O═C—O—C*—H system should be expected. However, in the investigated, asymmetrically substituted derivatives, the almost eclipsed O═C—O—C*—H bond system, if present, appears only in one of two halves of the molecule (Tables 3 and 4) and the eclipsing is in several cases far from ideal. From our investigations it also follows that such an eclipsed system is not present in the symmetrically substituted derivatives (Rychlewska & Warżajtis, 2000*b*).

Besides the dipolar interactions, which play a significant role in stabilizing the molecular conformation, an antiperiplanar conformation of the O═C(NH$_2$)—C*O and O═C(NHMe)—C*O moieties is stabilized by intramolecular hydrogen bonds of the N—H$_{trans}$···O type, which close the five-membered ring [the *S*(5) motif; Bernstein *et al.*, 1995, and references therein]. This type of intramolecular hydrogen bond is observed, without exception, in all derivatives containing a primary or secondary amide substituent (BOH1, BOH2, BN13, BN23 and BOM1; Fig. 3, Table 6).

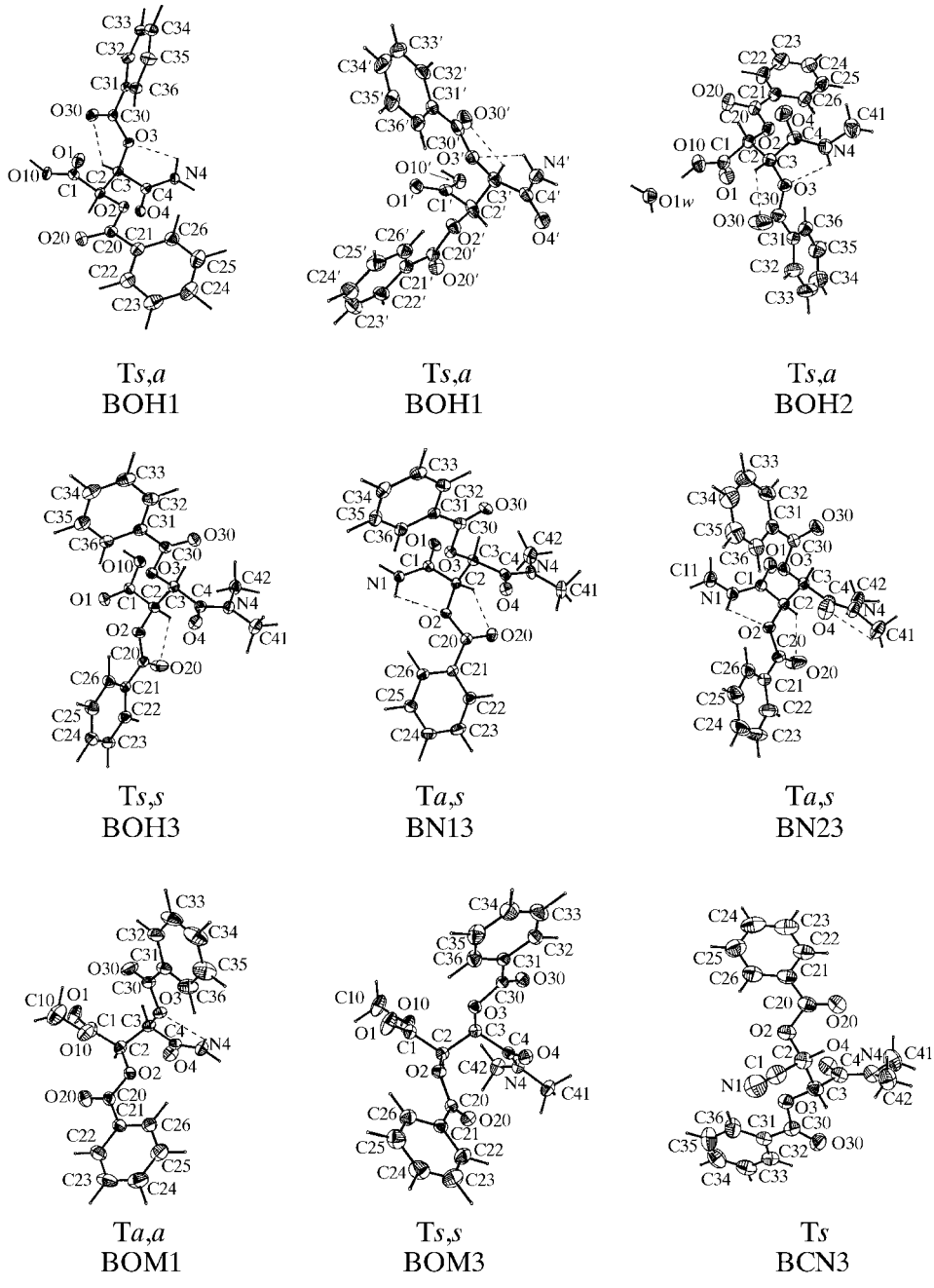

Figure 3
*ORTEP*II (Johnson, 1976) drawings of the asymmetric units. Thermal ellipsoids are drawn at the 40% probability level. The molecular conformation is stabilized by intramolecular hydrogen bonds (dashed lines) and attractive dipole–dipole interactions. Note the conformational changes around Csp^3—Csp^2 bonds that take place upon substitution. The *Ts*,*a* conformation of BOH1 (two independent molecules) and BOH2 illustrates a change in conformation when the carboxyl group is replaced by a primary (BOH1) or secondary (BOH2) amide function. The *Ts*,*s* conformation of BOH3 and the *Ta*,*s* conformation of BN13 and BN23 illustrate that tertiary amides adopt the *s* conformation independent of the substituent at the other end of the molecule. The *Ta*,*a* conformation of BOM1 and the *Ts*,*s* conformation of BOM3 show that the methylester group adjusts its orientation to mimic the conformation adopted by the other terminal group.

3.1.4. Planarity and relative orientation of the benzoyloxy substituents. While interpreting the spectroscopic results it is often assumed that the benzoate group is planar. In the crystal structure, however, an involvement of the benzoyloxy carbonyl groups in strong intermolecular dipolar interactions (BOM3 and BCN3, *see below*) or as intra- and intermolecular hydrogen-bond acceptors

Table 3
Selected torsion angles (°).

	C1—C2—C3—C4	O1═C1—C2—O2	O4═C4—C3—O3	H2—C2—O2—C20	C2—O2—C20═O20	O20═C20—C21—C22	H3—C3—O3—C30	C3—O3—C30═O30	O30═C30—C31—C32
BOH1	169.5 (2)	28.5 (4)	−173.7 (2)	−54	−3.7 (4)	5.4 (4)	13	−1.8 (4)	−38.1 (4)
	−173.2 (3)	11.9 (6)	161.6 (2)	−56	13.3 (4)	−4.8 (5)	24	−5.1 (4)	−14.4 (5)
BOH2	−172.8 (2)	27.5 (3)	177.8 (2)	−50	−4.6 (3)	−4.8 (3)	−1	−1.9 (3)	−13.2 (4)
BOH3	−178.9 (2)	−20.7 (3)	33.1 (3)	−9	1.6 (3)	−8.1 (4)	−48	−6.0 (3)	5.9 (4)
BN13	−173.7 (2)	−168.2 (2)	24.8 (4)	20	7.8 (4)	−5.7 (4)	−47	−1.3 (4)	−9.6 (4)
BN23	−178.1 (2)	176.3 (2)	18.2 (3)	7	−5.8 (4)	−11.2 (5)	−36	5.8 (4)	35.3 (4)
BOM1	−174.9 (2)	−158.0 (2)	−174.2 (2)	−53	1.5 (3)	−2.0 (4)	25	3.6 (3)	−3.4 (4)
BOM3	−175.4 (1)	15.8 (3)	20.9 (2)	25	9.5 (2)	25.7 (3)	−59	7.5 (2)	−11.2 (2)
BCN3	177.5 (3)		24.8 (4)	25	8.2 (4)	18.1 (5)	−52	6.0 (4)	−16.1 (5)

(BOH1, BOH2 and BN23; Table 6) significantly affects the overall planarity of the benzoyloxy substituent and thus disrupts a conjugation between the carbonyl and phenyl fragments. In the above-mentioned cases the O═C—C_{phenyl}—C_{phenyl} torsion angles range from 11.2 (5) to 38.1 (4)° (Table 3). Simultaneous significant deviations from planarity of both benzoyloxy substituents are observed in BN23. Moreover, in this molecule a relative orientation of the phenyl rings is substantially different than in any other molecule, the dihedral angle between the two planes being only 9.1 (2)°, while in the remaining structures it ranges from 42.7 (1) to 86.2 (1)°. It is not clear what might be the cause of this exceptional parallelism of the two phenyl rings, but clearly it cannot be solely a result of hydrogen bonds to benzoyloxy carbonyls, since such interactions are also observed in other crystal structures (Table 6). The partial lack of mesomerism in both benzoyloxy substituents in BN23 and the nearly parallel arrangement of both phenyl rings can be related with the very small value of the exciton Cotton effect ($\Delta\varepsilon$ = −2.8) observed for this compound in dioxane (Gawroński *et al.*, 1997). Nearly perpendicular orientation of the two phenyl rings is observed in BOM3 and BCN3 molecules which form isostructural crystals and are involved in strong intermolecular carbonyl dipole interactions (*see below*). In the remaining five compounds the interplanar angle ranges from 42.7 (1) to 63.3 (1)°.

3.1.5. Planarity of the *N*,*N*-dimethylamide groups. Table 5 lists the values of the out-of-plane deformation parameters observed in *N*,*N*-dimethylamide groups (Dunitz & Winkler, 1975). For compounds BOM3 and BCN3 the out-of-plane deformations are significantly larger than in any other derivative containing this group, the contribution of χ_N being much higher than the two other components, χ_C and τ. This can be accounted for by the repulsive interactions between N4 and O20, the N4···O20 distance being 3.209 (2) and 3.196 (4) Å, for BOM3 and BCN3, respectively. The fact that O20 approaches the amide nitrogen more closely in the two structures than in other *N*,*N*-dimethyltartramides might result from the carbonyl group at C20 being involved in dipolar interactions (see §3.2).

3.2. Intermolecular interactions

In the investigated series we observe an interplay between a variety of forces that govern the packing in crystals. These include hydrogen bonding between various hydrogen-bond functional groups, stacking of benzoyloxy substituents and carbonyl dipolar interactions.

3.2.1. Hydrogen bonding. Hydrogen-bond parameters are listed in Table 6. The stronger hydrogen-bonding donor groups are N—H in amide and *N*-methylamide, and OH in carboxylic group or water molecules. The hydrogen-bonding acceptor groups are >C═O groups of amide, ester and carboxyl residues, and water molecules.

3.2.2. The chain motifs. A general tendency in the investigated series is to form hydrogen bonds which connect molecules in a head-to-tail fashion. This is realised by joining molecules which are either related by a unit-cell translation or by a

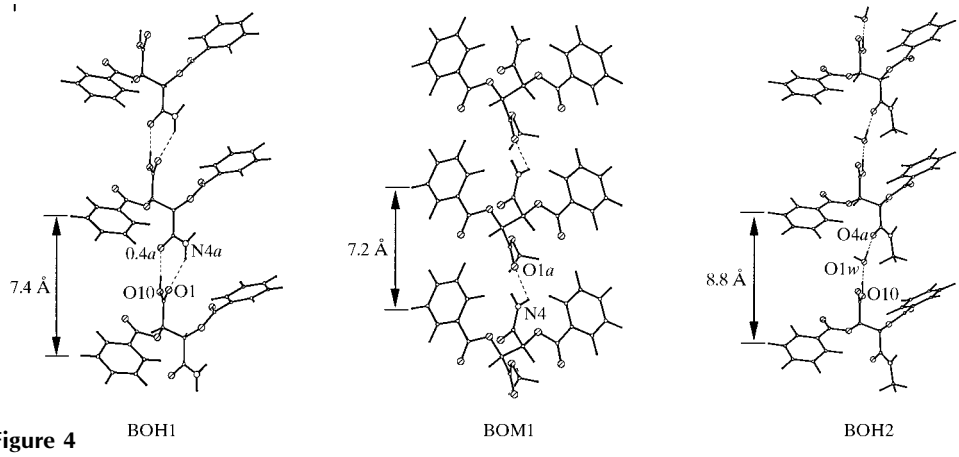

Figure 4
Various types of chains that join hydrogen-bonded molecules related by a unit-cell translation in a head-to-tail fashion. BOH1: two chains are shown, carboxyl···amide and amide···carboxyl; BOM1: amide···methyl-ester chain; BOH2: water mediated head-to-tail arrangement of translationally related molecules. *The following symbols appear in Figs. 4–8: ○ H atoms, ○ C atoms, ◯ N atoms and ▨ O atoms.

Table 4
Pseudo-torsion angles between CO/βC*H and CN/βC*H dipoles (°).

	C2—H2 C4═O4	C2—H2 C4—N4	C2—H2 C20═O20	C3—H3 C1—O10	C3—H3 C1═O1	C3—H3 C30═O30
BOH1	−6		−53	11		11
	−11		−40	19		19
BOH2	−3		−50	22		−3
BOH3		21	−7	−15		−50
BN13		16	26		7	−45
BN23		11	2		−5	−29
BOM1	2		−48		13	27
BOM3		19	31	18		−47
BCN3		14	31			−43

screw axis (Figs. 4 and 5, respectively). The former motif (Fig. 4) is analogous to the carboxyl···carboxyl chain present in the crystal structure of the parent (*R*,*R*)-tartaric acid (Okaya *et al.*, 1966), where the chain links translationally related molecules in a head-to-tail mode, parallel to the crystallographic axis of length 7.715 (3) Å. The motif not only appears in crystals of (*R*,*R*)-tartaric acid, but seems characteristic of the mode of packing of hydrogen tartrate anions and their *O*,*O*′-dibenzoyl derivatives (Brun & Larsen, 1999; Rychlewska & Warżajtis, 2000*a*, and references therein). A search through the CSD (Kennard & Allen, 1993) revealed 14 *O*,*O*′-dibenzoyl hydrogen tartrates that form hydrogen bonds as described above along the direction of the cell constant ranging from 7.287 (2) to 7.935 (2) Å. If one defines the C1–C4 direction as the direction of the molecular axis, then the set of 14 structures can be divided into two subgroups: one with the molecular axis forming the angle of approximately 20° with the unit-cell direction and the second with this angle not exceeding 5.5°. As expected, the unit-cell parameter increases as the angle between the two directions decreases. The average value for the unit-cell parameter in the first set amounts to 7.5 (1) Å and in the second set 7.84 (6) Å, which corresponds to an average angle of 22 (1) and 3 (1)°, respectively. In the investigated series, the translational head-to-tail arrangement is observed in BOH1, where each of the two independent molecules form such a chain along the *x* axis [*a* = 7.3930 (4) Å]. The angle between the molecular axis and the direction of propagation of the two chains formed by two independent molecules amounts to 14.6 (1) and 22.2 (1)°.

A topologically analogous chain motif can be seen in the crystal structure of BOM1 (Fig. 4). The *trans*-amide H atom acts as a donor to the ester carbonyl group that belongs to the translationally related molecule along the *x* direction [*a* = 7.193 (1) Å]. The carboxylic hydroxyl···amide carbonyl hydrogen bonds, present in the crystal structure of BOH1, although differing significantly in length, are both significantly shorter than the topologically similar amide···methylester carbonyl hydrogen bond formed in BOM1 (Table 6). This observation is just another manifestation of the well known generalization that ester carbonyls are much weaker acceptors than amide carbonyls.

The described chain motifs that join molecules related by a translation are depicted in Fig. 4, in which the water mediated head-to-tail arrangement of translationally related (*x*-direction) molecules is also shown [BOH2, *a* = 8.7977 (8) Å].

The head-to-tail arrangement of hydrogen-bonded molecules around a screw axis can be seen in the crystals of BOH3 and BN13, where the hydrogen bonds are, respectively, nearly parallel and perpendicular to the direction of the *C*(7) chain (Fig. 5). Clearly this difference in the direction of the hydrogen bond is a consequence of the different geometry of

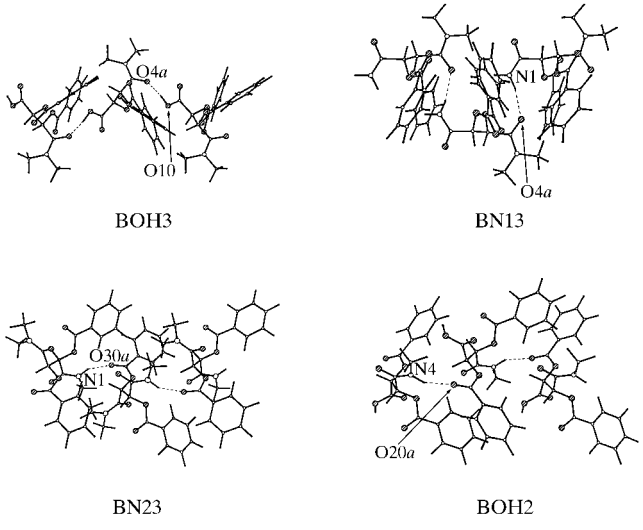

Figure 5
Various types of chains that join hydrogen-bonded molecules related by a twofold screw axis in a head-to-tail fashion. BOH3 and BN13 chose tertiary amide carbonyls as the best of the four possible carbonyl acceptors, while secondary amides in BN23 and BOH2 donate their N-H_{trans} protons to the distal benzoyloxy carbonyls.

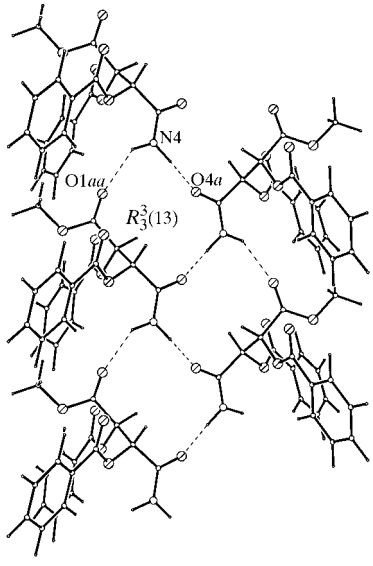

Figure 6
Combination of head-to-tail [*C*(7)] and head-to-head [*C*(4)] hydrogen-bond motifs in BOM1 gives rise to a ribbon consisting of fused $R_3^3(13)$ rings. Benzoyloxy substituents are situated on both sides of the ribbon, which are neighbours along *z* and are involved in sandwich stacking interactions (see Fig. 9).

Table 5
Out-of-plane deformation parameters (°) and torsion angles (°) about the C—N amide bond as observed in *N*,*N*-dimethylamide fragments (for a definition of the parameters see Dunitz & Winkler, 1975).

For the structure of BN33, see Rychlewska (1992).

	ω_1	ω_2	ω_3	ω_4	χ_C	χ_N	τ
BOH3	−179.6 (2)	−172.9 (2)	−2.8 (4)	10.3 (3)	3.2	9.9	−176.2
BN13	−171.3 (2)	−176.8 (3)	5.9 (5)	6.0 (5)	2.8	−2.7	−174.0
BN23	−175.3 (2)	−176.8 (3)	3.5 (4)	4.3 (4)	1.2	−0.3	−176.0
BN33	176.4 (2)	179.3 (3)	−4.1 (4)	−0.2 (4)	0.5	3.4	177.9
	−176.8 (3)	177.3 (3)	3.6 (4)	−3.1 (4)	−0.4	−6.3	180.3
BOM3	−176.5 (2)	168.8 (2)	4.3 (3)	−12.0 (2)	−0.8	−15.5	−183.8
BCN3	−178.2 (3)	168.9 (3)	2.0 (5)	−11.3 (5)	−0.2	−13.1	−184.6

proton donors [C(═O)OH *versus* C(═O)NH$_{trans}$]. It is worth noting that in the crystal structure of BN13 the N—H$_{cis}$ hydrogen does not act as a hydrogen-bond donor. The failure of the amide N—H donor to form a hydrogen bond in the presence of oxygen acceptors not involved in hydrogen-bonding is unusual though not unique.

In view of the fact that BN13 does not utilize its N—H$_{cis}$ hydrogen in hydrogen bonding and BN23 has this H atom replaced by a methyl group one might expect the two compounds to form a similar hydrogen-bond pattern. On the contrary, in BN23 the role of an acceptor in the N—H$_{trans}$···O═C hydrogen bond is taken over by a carbonyl group from a distal benzoyl substituent (O30). The benzoyl carbonyl group engaged as a hydrogen-bond acceptor is significantly out of the plane of the phenyl ring to which it is bonded (*see above*, Table 3). The hydrogen bond thus formed joins molecules into helical chains, described by the *C*(8) motif which might be viewed as topologically analogous, though not identical, to the described *C*(7) motif (Fig. 5).

Hydrogen bonds to benzoyloxy carbonyls are also seen in the crystal structures of BOH1 (Fig. 7) and BOH2 (Fig. 8), and in all these cases the amide group donates its *trans* H atom. In this respect it might be interesting to note that the carboxyl groups which always orient their H atom *cis* to the carbonyl group do not form hydrogen bonds with benzoyloxy carbonyls. Considering this, and in view of the fact that we were not able to obtain good quality crystals of the derivative with terminal COOH and COOMe groups (neither in the parent series, nor in the benzoylated series), we tend to conclude that carboxyl groups do not readily form hydrogen bonds with any ester carbonyl as an acceptor. Carboxyl groups also have difficulties packing efficiently in the presence of a methylamide substituent, but this is overcome by co-crystallization with the water molecule, a confining example being the crystal structure of BOH2 (*see below*) and its parent compound (Rychlewska & Warżajtis, 2000*a*).

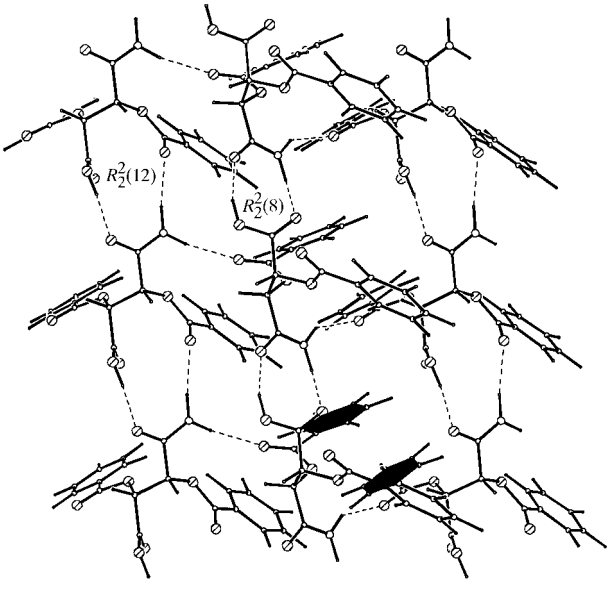

Figure 7
$R_2^2(8)$ ring pattern resulting from a head-to-tail acid/amide association and its modification, the $R_2^2(12)$ ring, which involves the benzoyl carbonyl as an acceptor (BOH1). The two chains of rings are further connected by hydrogen bonds to form the (010) layer perpendicular to the 20 Å direction. Phenyl groups that stick out of the layer are engaged in sandwich-stacking interactions.

3.2.3. The ring motifs. The head-to-head *C*(4) chains, typical for the self-association of amides, are formed only in BOM1 crystal structure. From our observations it follows that these chains appear only in those dibenzoylated derivatives in which the presence of a primary or secondary amide group is combined with such a molecular conformation that allows both terminal carbonyl substituents to be on the same side of the molecule. This creates conditions for the formation of fused hydrogen-bonded ring motifs. Obviously, the condition is easier to fulfil in the case of symmetrically substituted derivatives (Rychlewska & Warżajtis, 2000*b*). However, as mentioned earlier, the methylester group possesses an ability to rotate around the Csp^3—Csp^2 bond in order to adjust its conformation to that adopted by the amide substituent, situated at the other end of the molecule. This is illustrated in Fig. 3 for BOM1 and BOM3 molecules. Having methylester and amide carbonyl groups at the same side, the BOM1 molecule is able to use the two carbonyls as hydrogen-bond acceptors and to form hydrogen-bonded $R_3^3(13)$ ring motifs (Fig. 6). As a result of joining two ends of the same molecule *via* two neighboring amide residues, double molecular ribbons are generated that extend along a twofold screw axis. Within the ribbon one can distinguish *C*(4) chains composed exclusively of the amide units related by a twofold screw axis and stabilized by π-cooperativity and *C*(7) chains formed by the isolated N—H(amide)···O═C(methylester) hydrogen bonds. The N—H···O═C(amide) bonds are much stronger (as judged from the H···acceptor distances) than the isolated N—H···O═C(methylester) bonds (Table 6), which is presumably a result of both the presence of π-cooperativity in the C(4) chain, and the greater hydrogen-bond accepting ability of the

amide carbonyl compared with the ester carbonyl. Outside the ribbon the molecules form stacked dimers (*see below*).

The other rings that constitute the hydrogen-bond building blocks are the classical acid/amide $R_2^2(8)$ dimers (Leiserowitz, 1976) and analogous to them the $R_2^2(12)$ rings which are formed in the crystal structure of BOH1 by combining together, on a binary level, two $C(7)$ chains joining the molecules in a head–to–tail mode (Fig. 7). Formation of the $R_2^2(8)$ acid/amide dimer takes place at the expense of the co-planarity of the carboxyl group with proximal C*—O bonds (Table 3). However, the hydrogen-bond parameters are favorable, both H···acceptor distances being much shorter than in the $R_2^2(12)$ ring, formed by combining together the acid···amide and the N—H_{cis}···O═C(benzoyloxy) chains (Table 6).

3.2.4. Pleated sheets. Layers consisting of hydrogen-bonded molecules and situated perpendicular to the longest unit-cell axis of approximately 20 Å seem to be a characteristic element of the packing of the dibenzoylated tartramic acids BOH1 and BOH2. In BOH1 the layers form as a result of connecting together, by N—H_{trans}···O═C(benzoyl) hydrogen bonds, the two sets of chains mentioned above, *e.g.* the chains of $R_2^2(8)$ and $R_2^2(12)$ rings, respectively.

In BOH2 methyl substitution blocks the N—H_{cis} donor group, thus preventing the formation of hydrogen-bonded rings analogous to those formed by BOH1 molecules. However, in BOH2 one can distinguish a dimeric unit within which the screw-axis-related molecules (symmetry operation $-x, \frac{1}{2}+y, \frac{3}{2}-z$) join together by five different types of interactions, *i.e.* water···carboxyl, water···amide, amide···O═C(benzoyl), and C—H···O═C(amide) hydrogen bonds (Table 6), and sandwich stacking interactions (Fig. 8). These dimeric units which are translationally related along x are connected into chains by carboxyl···water···amide hydrogen bonds [$C_2^2(9)$ pattern designator] and those which are screw-axis related along y are connected into homodromic $C_2^2(6)$ chains. A combination of the two patterns gives infinite (001) layers of hydrogen-bonded molecules (Fig. 8).

3.2.5. Carbonyl–carbonyl dipole interactions. Symmetrical benzoylation and replacement of carboxyl groups in (*R*,*R*)-

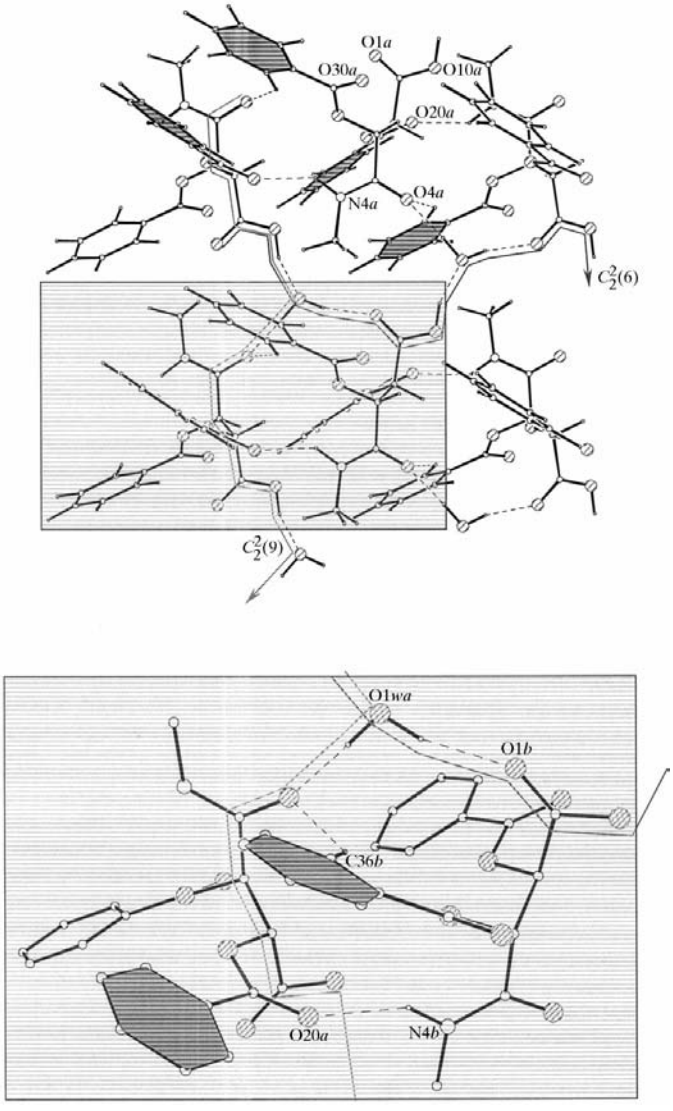

Figure 8
BOH2: layers of hydrogen-bonded molecules arranged in a close-packed fashion lie perpendicular to the 20 Å direction. Phenyl rings that stick out of the hydrophilic layer are engaged in sandwich-stacking interactions. A highlighted fragment of the layer illustrates five types of interactions between two neighbouring molecules: sandwich stacking and N—H···O═C(Bz), O*W*—H···O═C(carboxyl), O*W*—H···O═C(amide), and C—H···O═C(amide) hydrogen bonds (only H atoms involved in hydrogen bonds are shown). The unit is further linked *via* water molecules in two directions: the x direction [units related by translation, $C_2^2(9)$ pattern] and the y direction [units related by a twofold screw axis, $C_2^2(6)$ homodromic chain].

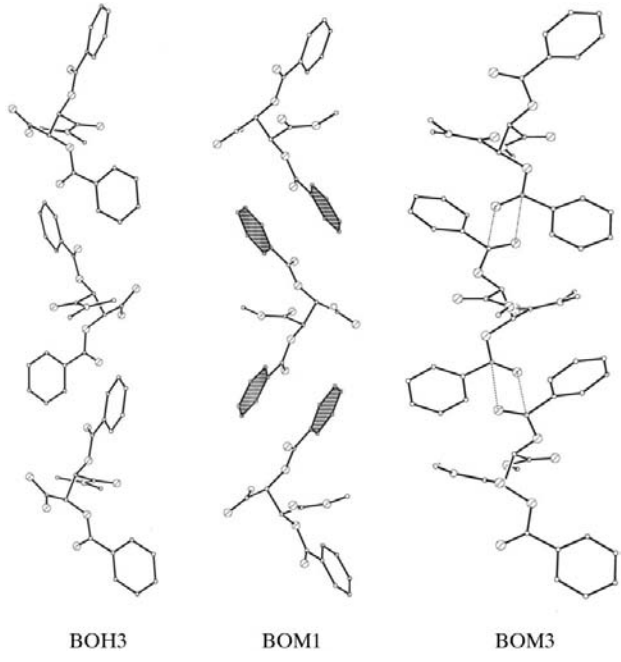

Figure 9
BOH3: Molecular shape dictates the arrangement of molecules along a twofold screw axis of length ∼18–19 Å. BOM1: slightly modified molecular arrangement leads to sandwich stacking. BOM3: another small variation gives rise to carbonyl dipolar interactions (dotted lines) and shortening of the unit-cell parameter to 14 Å (also observed in BCN3 which is isostructural with BOM3). H atoms have been omitted for clarity.

Table 6
Hydrogen-bond geometry of the *O*,*O*′-dibenzoyl derivatives of (*R*,*R*)-tartaric acid, asymmetrically substituted by ester, amides and nitriles.

Intramolecular hydrogen bonds have been marked with asterisks; carbon···oxygen hydrogen bonds are in italics; C—H, N—H and O—H distances have been standardized to values 1.10, 1.03 and 0.97 Å, respectively. $^+$ designates atoms constituting minor components in a disorder model.

Compound		*D*···*A* (Å)	H···*A* (Å)	*D*—H···*A* (°)	Symmetry operations on *A*
BOH1	N4—H42···O3*	2.639 (3)	2.19	104	
	N4′—H42′···O3′*	2.643 (3)	2.24	102	
M = 357.31	*C3—H3···O30**	*2.691 (3)*	*2.22*	*103*	
m.p. = 431–435 K	*C3′—H3′···O30′**	*2.709 (4)*	*2.29*	*100*	
	O10—H10···O4	2.573 (3)	1.60	175	$-1+x, y, z$
	O10′—H10′···O4′	2.759 (4)	1.81	164	$1+x, y, z$
	O10′—H10′···O1*W*$^+$	2.507 (8)	2.02	109	
	O10*A*$^+$···O1′	2.683 (9)			
	O10*A*$^+$···O1*W*$^+$	2.549 (11)			
	O1*W*$^+$···O1	2.857 (8)			$1+x, y, 1+z$
	O1*W*$^+$···O4′	2.590 (8)			$1+x, y, z$
	N4—H41···O1	2.870 (3)	1.95	147	$1+x, y, z$
	N4—H42···O20′	2.946 (3)	2.04	146	$x, y, -1+z$
	N4′—H41′···O30′	3.092 (3)	2.07	174	$-1+x, y, z$
	N4′—H42′···O30	3.126 (3)	2.16	156	
	C23—H23···O1′	*3.038 (6)*	*2.19*	*132*	$2-x, \frac{1}{2}+y, 1-z$
	C32—H32···O20	*3.205 (4)*	*2.42*	*127*	$1-x, -\frac{1}{2}+y, 1-z$
	C35—H35···O1′	*3.345 (5)*	*2.34*	*151*	$-1+x, y, -1+z$
BOH2	N4—H4···O3*	2.671 (2)	2.20	106	
H_2O	*C3—H3···O30**	*2.640 (2)*	*2.11*	*106*	
	O10—H10···O1*W*	2.569 (2)	1.64	158	
M = 389.35	O1*W*—H1*W*···O4	2.709 (2)	1.74	177	$1+x, y, z$
m.p. = 397–405 K	O1*W*—H2*W*···O1	2.898 (2)	1.95	166	$1-x, -\frac{1}{2}+y, \frac{3}{2}-z$
	N4—H4···O20	2.900 (2)	2.02	142	$-x, \frac{1}{2}+y, \frac{3}{2}-z$
	C22—H22···O30	*3.326 (3)*	*2.51*	*130*	$\frac{1}{2}-x, 1-y, -\frac{1}{2}+z$
	C36—H36···O4	*3.356 (3)*	*2.50*	*133*	$-x, \frac{1}{2}+y, \frac{3}{2}-z$
BOH3	*C2—H2···O20**	*2.647 (3)*	*2.15*	*104*	
	O10—H10···O4	2.625 (2)	1.66	175	$-x, -\frac{1}{2}+y, \frac{1}{2}-z$
M = 385.36	*C25—H25···O30*	*3.403 (3)*	*2.42*	*147*	$-x, \frac{1}{2}+y, \frac{1}{2}-z$
m.p. = 426–429 K	*C32—H32···O20*	*3.509 (4)*	*2.43*	*166*	$\frac{1}{2}-x, -y, -\frac{1}{2}+z$
	C42—H422···O1	*3.246 (3)*	*2.15*	*173*	$1+x, y, z$
BN13	N1—H12···O2*	2.696 (3)	2.27	103	
	*C2—H2···O20**	*2.646 (4)*	*2.19*	*102*	
M = 384.38	N1—H12···O4	2.978 (3)	2.13	139	$\frac{1}{2}+x, -\frac{3}{2}-y, -2-z$
m.p. = 425–427 K	*C22—H22···O30*	*3.514 (4)*	*2.44*	*166*	$-\frac{1}{2}-x, -2-y, -\frac{1}{2}+z$
	C26—H26···O4	*3.464 (4)*	*2.37*	*172*	$\frac{1}{2}+x, -\frac{3}{2}-y, -2-z$
	C41—H411···O1	*3.283 (4)*	*2.51*	*126*	$-1+x, y, z$
	C42—H423···O1	*3.412 (4)*	*2.45*	*145*	$-\frac{1}{2}+x, -\frac{5}{2}-y, -2-z$
BN23	N1—H1···O2*	2.668 (2)	2.21	105	
	*C2—H2···O20**	*2.657 (3)*	*2.15*	*105*	
M = 398.41	*C41—H413···O4**	*2.744 (4)*	*2.32*	*100*	
m.p. = 474–476 K	N1—H1···O30	2.892 (3)	1.97	147	$-x, \frac{1}{2}+y, 1-z$
	C23—H23···O20	*3.302 (4)*	*2.36*	*142*	$1-x, \frac{1}{2}+y, 2-z$
	C41—H413···O1	*3.202 (3)*	*2.32*	*136*	$1+x, y, z$
BOM1	N4—H42···O3*	2.621 (2)	2.18	103	
	N4—H42···O1	2.918 (2)	2.29	118	$1+x, y, z$
M = 371.34	N4—H41···O4	2.835 (2)	1.81	173	$\frac{1}{2}+x, \frac{3}{2}-y, 1-z$
m.p. = 396–399 K	*C25—H25···O20*	*3.236 (4)*	*2.48*	*125*	$1+x, y, z$
	C32—H32···O20	*3.394 (4)*	*2.41*	*148*	$-\frac{1}{2}-x, 1-y, \frac{1}{2}+z$
	C33—H33···O4	*3.576 (3)*	*2.50*	*164*	$-x, -\frac{1}{2}+y, \frac{3}{2}-z$
BOM3	*C10—H103···O4*	*3.452 (2)*	*2.45*	*150*	$x, y, -1+z$
	C23—H23···O4	*3.373 (3)*	*2.29*	*167*	$1-x, -\frac{1}{2}+y, 2-z$
M = 399.39	*C42—H422···O1*	*3.335 (2)*	*2.48*	*133*	$1+x, y, z$
m.p. = 368–376 K					
BCN3	*C24—H24···O4*	*3.235 (5)*	*2.35*	*136*	$1-x, -\frac{1}{2}+y, 2-z$
	C35—H35···O30	*3.336 (6)*	*2.24*	*176*	$-1+x, y, z$
M = 366.36					
m.p. = 372–374 K					

tartaric acid by methyl ester, tertiary amide or nitrile groups limits possible hydrogen bonds to only C—H···O interactions (Table 6). It might be expected that in such derivatives the molecular orientation maximizing electrostatic interactions will be favoured and that these interactions might be relevant to crystal packing. A spectacular example of the presence of such attractive interactions is provided in crystals of BOM3 and BCN3. The crystals are isostructural, and in both crystal structures screw-diad-related C═O groups from two different benzoyl substituents are arranged antiparallel (Fig. 9). In the crystal structure of BCN3 the interacting molecules are related by an approximate center of inversion situated at 0.5, 0.4, 0.5, but the pairs of 'related atoms' are not chemically identical. The distance between the C═O midpoints and the angle between the interacting dipoles is 3.067 (2) Å and 9.2 (2)° in BOM3, and 3.107 (4) Å and 11.5 (3)° in BCN3. Table 7 lists two C···O contacts, four contact angles and two C═O···C═O torsion angles for each of the two structures. For the planar antiparallel arrangement of the interacting dipoles the torsion angles should be close to zero and the valency angles close to 90°. The observed values are close to a perfect rectangular antiparallel dimer and suggest strong dipole/dipole interactions. According to Allen *et al.* (1998) an attractive interaction energy for such system amounts to −22.3 kJ mol^{-1}, which is comparable to the energies of medium-strength hydrogen bonds. As a result of such electrostatic interactions, O20 in BOM3 is significantly out of plane of the phenyl ring to which it is bonded, the deviation being 0.501 (4) Å, while O30 is out of

Table 7
Parameters describing mutual orientation of interacting carbonyl dipoles (Å, °).

	BOM3	BCN3
C20···O30^{i}	2.994 (2)	3.061 (4)
O20···C30^{i}	3.142 (2)	3.158 (4)
C20═O20···C30^{i}	94.6 (1)	89.3 (2)
O20═C20···O30^{i}	84.8 (1)	90.3 (2)
C30^{i}═O30^{i}···C20	102.1 (1)	93.9 (2)
O30^{i}═C30^{i}···O20	78.0 (1)	85.6 (2)
C20═O20···C30^{i}═O30^{i}	9.0 (2)	11.3 (3)
C30^{i}═O30^{i}···C20═O20	9.5 (2)	11.7 (3)

this plane by 0.185 (3) Å. In the isostructural crystals of BCN3 these deviations are more symmetrical and amount to 0.305 (6) and 0.286 (6) Å for both C20 and C30 carbonyl substituents (also see Table 3).

3.2.6. Stacking interactions. Sandwich stacking interactions are observed in dibenzoyltartramic acids, BOH1 (Fig. 7) and BOH2 (Fig. 8), which form hydrogen-bonded layer structures perpendicular to the unit-cell direction of length ∼20 Å and in BOM1 which forms a double molecular ribbon of hydrogen-bonded molecules with phenyl rings on both sides (Fig. 9). The angle between the interacting phenyl substituents amounts to 5.0 (1) and 6.6 (1), and 14.8 (1) and 3.2 (1)° in two molecules of BOH1, BOH2 and BOM1, respectively. The perpendicular distance between the best plane through one of the rings and the midpoint of the other ring is 3.439 (2) and 3.458 (2), and 3.679 (2) and 3.503 (3) Å, respectively.

It is amazing to see how only a slight change in mutual orientation of molecules can cause a change in character of the intermolecular interactions (Fig. 9). One of the possible arrangements of the investigated molecules along the twofold screw axis, as dictated by their size and shape, is shown in Fig. 9 for BOH3. In the absence of any specific intermolecular interactions the molecules align approximately 18 Å along the axis in a close-packed fashion. A small reorientation of phenyl rings gives rise to sandwich stacking interactions (Fig. 9, BOM1), while mutual translation of the stacked molecules results in dipolar interactions between benzoyloxy carbonyls (Fig. 9, BOM3) and shortening of the unit-cell parameter to approximately 14 Å. Carbonyl dipolar interactions are observed in two isostructural crystals of BOM3 (Fig. 9) and BCN3, *see above*.

4. Conclusions

The results of the X-ray analysis of eight unsymmetrically substituted derivatives of *O*,*O*′-dibenzoyl-(*R*,*R*)-tartaric acid point to several factors that stabilize the molecular conformation and influence the packing in crystals.

(i) C*—H bonds at chiral centers show a tendency to orient parallel to one or two of the numerous C═O groups present in benzoylated molecules, thus allowing the mutual interactions of dipoles in the 1,3-position. In some cases the geometrical parameters allow the classification of such a contact as an intramolecular hydrogen bond of the C*—H···O═C type. The influence of these attractive forces on the molecular conformation might be significant owing to the fact that there might be a few such bond arrangements per molecule.

(ii) In addition to these CO/βC*H dipole/dipole interactions, the molecular conformation of primary or secondary amides is stabilized by intramolecular hydrogen bonds of the N—H···O—C* type.

(iii) Crystal packing is mostly governed by hydrogen bonds that join molecules in a head-to-tail fashion and supplemented by sandwich stacking interactions. Patterns characteristic for the self-association of amides are rather an exception.

(iv) Primary amides tend to form various types of ring patterns [($R_2^2(8)$, $R_2^2(12)$, $R_3^3(13)$], but overcrowding may prevent the N—H_{cis} donors from participation in hydrogen bonds.

(v) Secondary amides always choose to donate their proton to the distal benzoyloxy carbonyl which might be regarded as a manifestation of packing difficulties.

(vi) Carboxyl groups avoid hydrogen bonds with ester carbonyls as acceptors.

(vii) Molecules with an extended carbon-chain conformation that lack the 'classical' hydrogen-bond functional groups pack in such a way so as to maximize the intermolecular carbonyl dipole/dipole interactions.

(viii) The results indicate that antiparallel dipolar interactions play a significant role in stabilizing the molecular conformation and the crystal packing.

The authors wish to thank Professor J. Gawroński for providing the samples for X-ray analysis and for his stimulating interest in this work.

References

Allen, F. H., Baalham, C. A., Lommerse, J. P. M. & Raithby, P. R. (1998). *Acta Cryst.* B**54**, 320–329.
Bernstein, J., Davis, R. E., Shimoni, L. & Chang, N. L. (1995). *Angew. Chem. Int. Ed. Engl.* **34**, 1555–1573.
Brun, R. K. & Larsen, S. (1999). *Acta Cryst.* C**55**, 956–958.
Dunitz, J. D. & Winkler, F. K. (1975). *Acta Cryst.* B**31**, 251–263.
Gałdecki, Z., Kowalski, A. & Uszyński, L. (1995). *DATAPROC Data Processing Program.* Version 9. Kuma Diffraction, Wrocław, Poland.
Gawroński, J. & Gawrońska, K. (1999). *Tartaric and Malic Acids in Synthesis.* John Wiley and Sons, Inc., New York, NY, USA.
Gawroński, J., Gawrońska, K. & Rychlewska, U. (1989). *Tetrahedron Lett.* **30**, 6071–6074.
Gawroński, J., Gawrońska, K., Skowronek, P., Rychlewska, U., Warżajtis, B., Rychlewski, J., Hoffmann, M. & Szarecka, A. (1997). *Tetrahedron*, **53**, 6113–6144.
Hommeltoft, S. I., Cameron, A. D., Shacleton, T. A., Fraser, M. E., Fortier, S. & Baird, M. C. (1986). *Organometallics*, **5**, 1380–1388.
Houk, K. N., Eksterowicz, J. E., Wu, Y.-D., Fuglesang, C. D., Mitchell, D. B. (1993). *J. Am. Chem. Soc.* **115**, 4170–4177.
Jaskólski, M. (1982). *Collected Abstracts, Symposium on Organic Crystal Chemistry*, edited Z. Kałuski, p. 70. UAM, Poznań, Poland.

Johnson, C. K. (1976). *ORTEP*II. Report ORNL-5138. Oak Ridge National Laboratory, Oak Ridge, Tennessee, USA.
Kennard, O. & Allen, F. H. (1993). *Chem. Des. Autom. News*, **8**, 1, 31–37.
Kroon, J. (1982). *Conformational aspects of Meso-Tartaric Acid*, edited by J. F. Griffin and W. L. Duax, pp. 151–163. Buffalo, NY: Elsevier Biomedical.
Kuma Diffraction (1991). *KM*-4 *User's Guide*, Version 3.2. Kuma Diffraction Instruments GmbH, Wrocław, Poland.
Kuma Diffraction (1999*a*). *KM*4*CCD Software*, Version 1.162. Kuma Diffraction Instruments GmbH, Wrocław, Poland.
Kuma Diffraction (1999*b*). *KM*4*RED Software*, Version 1.162. Kuma Diffraction Instruments GmbH, Wrocław, Poland.
Lehmann, M. S. & Larsen, F. K. (1974). *Acta Cryst.* A**30**, 580–584.
Leiserowitz, L. (1976). *Acta Cryst.* B**32**, 775–802.
Liang, C., Ewing, C. S., Stouch, T. R. & Hagler, A. T. (1994). *J. Am. Chem. Soc.* **116**, 3904–3911.
Nishio, M., Hirota, M. & Umezawa, Y. (1998). *The CH/π Interaction. Evidence, Nature and Consequences.* Wiley-VCH: New York, Chichester, Weinheim, Brisbane, Singapore, Toronto.
Okaya, Y., Stemple, N. R. & Kay, M. I. (1966). *Acta Cryst.* **21**, 237–243.
Rychlewska, U. (1992). *Acta Cryst.* C**48**, 965–969.
Rychlewska, U. & Warżajtis, B. (2000*a*). *Acta Cryst.* B**56**, 833–848.
Rychlewska, U. & Warżajtis, B. (2000*b*). To be published.
Rychlewska, U., Warżajtis, B., Hoffmann, M. & Rychlewski, J. (1997). *Molecules*, **2**, 106–113.
Sheldrick, G. M. (1990). *Acta Cryst.* A**46**, 467–473.
Sheldrick, G. M. (1997). *SHELXL*97. University of Göttingen, Germany.
Siemens (1989). *Stereochemical Workstation Operation Manual*, Release 3.4. Siemens Analytical X-ray Instruments Inc., Madison, Wisconsin, USA.
Syntex (1973). *Syntex* $P2_1$ *Software.* Syntex Analytical Instruments, Cupertino.